Characterization of Model Anaerobic Adhesive Cure Using Real-Time Fourier Transform Infrared Spectroscopy and Dielectric Spectroscopy

BRENDAN P. MCGETTRICK,[1] JAGDISH K. VIJ,[1,*] and CIARAN B. MCARDLE[2]

[1]Department of Microelectronics and Electrical Engineering, University of Dublin, Trinity College, Dublin 2, Ireland, and [2]Loctite (Ireland) Ltd., Research and Development Laboratories, Chemical and Materials Science Department, Whitestown Industrial Estate, Tallaght, Dublin 24, Ireland

SYNOPSIS

A technique has been developed based on Fourier transform infrared spectroscopy (FTIR) in the attenuated total reflectance (ATR) mode, which is suitable for the investigation of the heterogeneous cure of surface-initiated redox polymerizations in thin and thick bondline situations. The results of the investigations into the surface-catalyzed and anaerobically promoted cure of some model adhesives using this method are reported. The systems under investigation were designed to exhibit different levels of cure heterogeneity or "cure through volume" (CTV) so that the influence of the bondline thickness and the formulation variables may be assessed. The analysis of the data provides evidence that supports our concept of the heterogeneous cure distribution existing in the form of a cure gradient. This concept of a cure gradient is developed further using dielectric spectroscopy. Here the cure gradient is characterized in terms of the parameters obtained using an empirical equation to fit the dielectric relaxation data. The results obtained using the infrared and dielectric spectroscopic methods are in satisfactory agreement and are shown to be most informative in characterizing and quantifying the CTV performance of the model anaerobic adhesives. © 1994 John Wiley & Sons, Inc.

INTRODUCTION

Real-time Fourier transform infrared spectroscopy (RT-FTIR) as a means of examining cure was first proposed by Decker and Moussa.[1] The method allows the continuous, nondestructive monitoring of polymerization at the molecular level, and it has been widely used in radiation curing studies.[1-8] The polymerization process may be followed by observing changes in the infrared intensities of the signals associated with specific functional groups. Thus, for example, in the case of vinyl polymerization the chemical reaction may be monitored by observing the absorption peaks characteristic to the carbon–carbon double bond as a function of cure time. The absorption peaks at 1634 and 810 cm^{-1} are specific to the C=C stretching and the C—H deformation mode of the vinyl group, respectively. The decrease in intensity of these peaks as cure progresses may be attributed to the gradual disappearance of the vinyl double bond.[1,3-5,8-11] Thus, the progress of vinyl polymerization may be spectroscopically recorded in real time as cure ensues.

We report the use of RT-FTIR using the attenuated total reflectance (ATR) technique.[12] ATR is widely used in the depth profiling and the characterization of polymer interfaces.[13-17] The fundamental principle of ATR is illustrated in Figure 1. A beam of radiation entering a crystal or internal reflection element (IRE) will undergo total internal reflection when the angle of incidence between the sample and the IRE is greater than the critical angle, which is a function of the refractive indices of the two surfaces. At the point of reflection the infrared beam penetrates slightly into the rarer medium (sample), and it is displaced a distance D upon re-

* To whom correspondence should be addressed.

Journal of Applied Polymer Science, Vol. 52, 737–746 (1994)
 CCC 0021-8995/94/060737-10

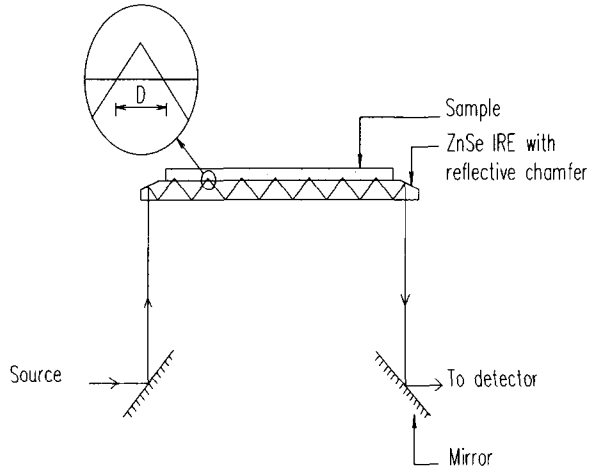

Figure 1 Illustration of the attenuated total reflectance (ATR) technique. The inset illustrates the penetration of the evanescent wave into the sample and the displacement D of the infrared beam upon total internal reflection.

flection. This results because of an electromagnetic disturbance in the sample. The disturbance is an evanescent wave arising from the interference of the incident and the reflected waves. It exhibits the same frequency as the incident wave, and its electric field amplitude falls off exponentially with the distance from the IRE–sample interface as in Eq. (1):

$$E = E_0 \exp(-Z/d_p) \tag{1}$$

where E is the electric field amplitude, E_0 is the electric field amplitude at the IRE–sample interface, and Z is the decay constant. The distance required for the electric field amplitude to fall to e^{-1} of its value at the interface, d_p, is given by Eq. (2):

$$d_p = \frac{\lambda}{2\pi n_1 (\sin^2\theta - n_{21}^2)^{1/2}} \tag{2}$$

where λ is the irradiation wavelength in vacuum, θ is the angle of incidence, and n_{21} is the ratio of the refractive indices of the sample and the IRE. n_1 is the refractive index of ZnSe crystal. d_p is of the order of several microns. Coupling to the evanescent wave extracts energy from it and makes the reflection less than total. In the case of attenuated total reflectance (ATR) energy is absorbed by the sample and there is an energy loss that may be detected.

The use of dielectric spectroscopy in the study of the cure process in epoxies cured with amines has been extensively reported in the literature.[18–26] Some of the present authors have recently shown the method to be one of the most useful techniques for the study of cure in anaerobic acrylic adhesives.[27–29] In the present study the physical properties of isothermally cured anaerobic adhesive samples are described by analyzing the observed dielectric relaxation data in terms of the Cole–Cole empirical expression.[30]

The object of this work is to characterize the cure of surface-initiated model anaerobic acrylic adhesives,[31–34] which are formulated to exhibit varying levels of cure heterogeneity or cure through volume (CTV). While the term *anaerobic* is meant to imply that such adhesives will cure in the absence of air, for example, between closely mating substrates, it is actually redox chemistry initiated by metallic species on the substrates that is responsible for the vast majority of their room temperature, isothermal cure. The curing mechanism of anaerobic acrylic adhesives has been described elsewhere.[29,31–34]

EXPERIMENTAL

Materials

Two stable model anaerobic acrylic adhesive samples, CTV1 and CTV2, were formulated. CTV1 and CTV2 are code names and do not imply any specific characteristics. These were designed in the Research and Development Laboratories of Loctite (Ireland) Ltd. to exhibit different levels of CTV performance. The formulations were composed of a polyfunctional urethane methacrylate resin base, acrylic monomers and diluents, cumene hydroperoxide, saccharin, stabilizers, and an accelerating additive. The low CTV formulation, CTV1, and the high CTV formulation, CTV2, contained different levels of essentially the same components. The accelerating additive was, however, different for each system. CTV1 employed acetyl phenyl hydrazine (APH) while the additive used in CTV2 is of a proprietary nature and is referred to as BPH.[29] The nature of the accelerating additive in CTV2 necessitated the use of a substrate primer to achieve cure. The substrate primer was a commercially available copper-salt-based activator, known as Primer N (Loctite UK, Welwyn Garden City). This primer was not employed for CTV1 because of the experimental difficulties associated with RT monitoring of a vastly accelerated cure.[28] It is important to note that these curing systems were selected because they simply exhibit significantly different levels of CTV. They are thus suitable for study in the development of analytical methods for the study of the CTV phenomenon. The reasons for the improved CTV per-

formance in CTV2 with Primer N have been previously discussed by us[29] and will not be dealt with here.

RT-FTIR Measurements

A Bio-Rad (Cambridge, MA) FTS-60A system employing a liquid-nitrogen-cooled MCT detector and a Graseby Specac 11050 overhead ATR accessory with a zinc selenide (ZnSe) internal reflection element (IRE) was used. Figure 1 illustrates the general configuration of the ATR accessory. Figure 2 illustrates the setup of the ATR accessory used for the investigations. The spacing between the iron substrate and the crystal was set using uniform crosslinked polystyrene microbeads with well-characterized diameters (Bangs Laboratories Inc, Carmel, Indiana, USA). The iron substrate was primed using Primer N in the case of the CTV2 formulation (see above). It is important to emphasize that the cure emanates from the iron substrate "downward" in the direction of the ZnSe IRE. Since d_p is of the order of microns the spectra obtained correspond to the sample material adjacent to the crystal, that is, farthest from the substrate. Since the cure in anaerobic adhesives is catalyzed by ferric and cupric species,[28,31-34] it was assumed that negligible cure occurs at the crystal (ZnSe)-adhesive interface due to any crystal-promoted chemical reactions or due to any depletion of reaction inhibiting oxygen. Also the possibility of cure activated by thermal energy from the infrared beam[35] was not taken into consideration. Thus the progress of cure triggered from the primed substrate and emanating through the bulk adhesive toward the IRE was monitored by looking "upward" into the bondline as in Figure 2. This method was effectively equivalent to observing the chemical changes occurring from within the bulk adhesive, that is, from the halfway point in the bondline. This feature was ideal for our investigations, which concern the characterization of the cure through bondline thickness or the cure through volume (CTV) performance of surface-initiated model anaerobic adhesive formulations. Furthermore, it contrasts our earlier work,[27-29] which essentially considers heterogeneous cure throughout the bondline as a whole using dynamic mechanical thermal analysis (DMTA) and dielectric spectroscopy.

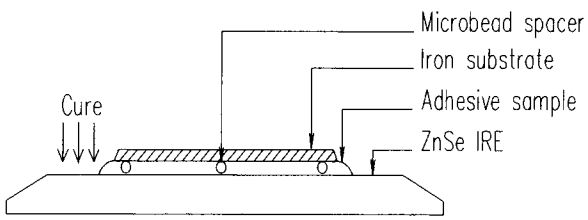

Figure 2 The experimental setup employed for the study of the cure using RT-FTIR in the ATR mode.

The infrared spectra were collected at various intervals up to a total cure time t of 11 h. The CTV1 and CTV2 model formulations were investigated at different adhesive layer thicknesses. The progress of acrylic polymerization was followed by monitoring the changes in the intensities of the peaks corresponding to the disappearance of the C=C carbon–carbon double bonds. The absorption peak at 815 cm^{-1}, which is specific to the C—H deformation mode of the vinyl group, was chosen for the calculations as it was much stronger than that observed at 1635 cm^{-1}. The value of d_p at 815 cm^{-1} was estimated to be 8 μm. Shrinkage in acrylic polymerizations is well known,[36,37] and certain measures were taken to correct for any shrinkage effects in the spectra. One such measure was to integrate the area under the peak instead of relying solely on the peak intensities for the calculations so as to reduce experimental deviation. The areas of the peaks of interest were calculated using a computer software package that fits a weighted sum of Gaussian and Lorentzian curves to the band profile. Furthermore, an internal standard was used to correct for shrinkage. The C=O acrylic ester carbonyl stretch at 1730 cm^{-1} was chosen for the latter calculations since the carbonyl groups do not participate in the polymerization and are hence not depleted.[38]

The degree of cure α was calculated at various intervals using Eq. (3):

$$\alpha = \left(\frac{A_0 - A_t}{A_0}\right) \times 100\% \qquad (3)$$

where A_0 is the ratio of the area of the C—H vinyl deformation peak between 840 and 790 cm^{-1} and the area of the C=O carbonyl stretch peak between 1780 and 1660 cm^{-1} at cure time $t = 0$; and A_t is the ratio of the same peaks at a later cure time t. Plots of the degree of cure α versus the cure time t were constructed for CTV1 and CTV2 at various thicknesses, d. From this data plots of α versus d for a cure time t of 11 h were obtained for each model formulation.

Dielectric Spectroscopy Measurements

The measurements were performed using a system comprising a Schlumberger SI 1255 frequency response analyzer interfaced to a Chelsea dielectric

interface (Dielectric Instrumentation, Holt Heath, Worcestershire, England) and a Hewlett-Packard Vectra QS/165 PC. The samples consisted of the adhesive contained in between flat-tempered iron electrodes of 30 mm in diameter and 0.5 mm in thickness (Goodfellow Metals, Cambridge, UK; FE000405/11). The electrodes were prepared with a copper primer called Primer N in the case of the CTV2 formulation (see above). The electrode spacing was set using uniform crosslinked polystyrene microbeads with well-characterized diameters (Bangs Laboratories Inc., Carmel, USA). This disposable arrangement was placed in a three-terminal dielectric cell similar to that designed by Kremer et al.[39] The measurements were made at room temperature.

Measurements of the real part ε' and the imaginary part ε'' of the complex permittivity $\varepsilon(\omega)$ in the frequency range 1 Hz to 100 kHz were made on samples of CTV1 and CTV2 of various thicknesses. A conductivity subtraction technique was used to correct for the dc conductivity.[40] The corrected data was fitted to an empirical equation. Plots of the measured dissipativity ε'' versus frequency f along with the fitted data are presented in Figures 8 and 9. The values obtained for the fitting parameters are presented in Table II.

RESULTS AND DISCUSSION

FTIR Measurements

This study is concerned solely with the end properties of the isothermally cured samples and thus, the parameters governing the reaction kinetics have not been calculated from the infrared data. Plots of the conversion α versus the cure time t for samples of CTV1 and CTV2 of thickness d are presented in Figures 3 and 4, respectively. CTV1 and CTV2 are the low and high CTV performance formulations, respectively. It is assumed that no significant further cure has taken place after a cure time of 11 h (this was verified by subsequent measurements). The intersection of an isochrone (line at constant time) of t = 11 h drawn on the graphs of Figures 3 and 4 yields data that may be used to construct a plot of the essentially maximum conversion α versus d at t = 11 h (Fig. 5).

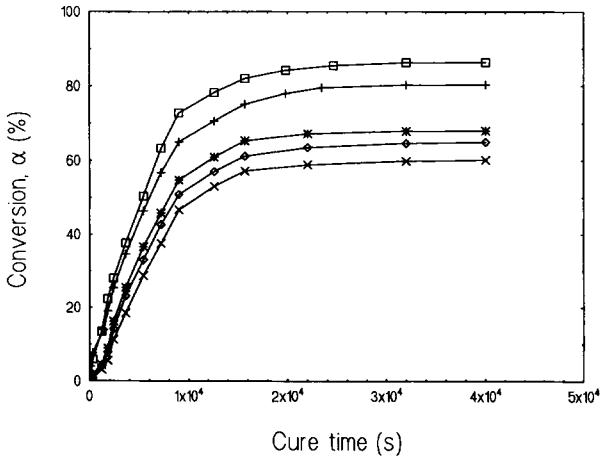

Figure 4 Plots of the degree of conversion α as a function of the cure time t for the CTV2 formulation at different sample thicknesses: (□) 101 μm, (+) 153 μm, (∗) 384 μm, (◇) 511 μm, and (×) 805 μm.

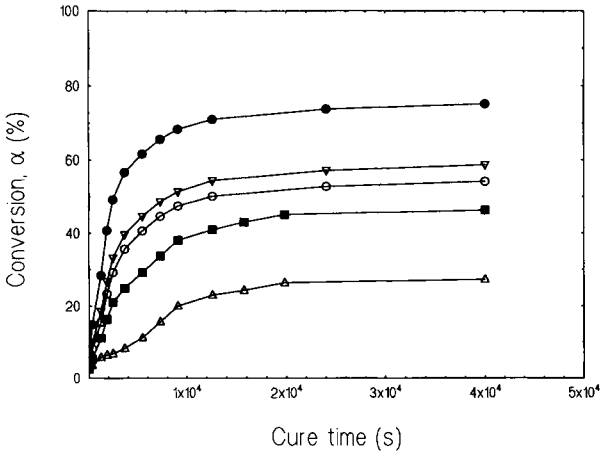

Figure 3 Plots of the degree of conversion α as a function of the cure time t for the CTV1 formulation at different sample thicknesses; (●) 94 μm, (▽) 241 μm, (○) 450 μm, (■) 603 μm, and (△) 801 μm.

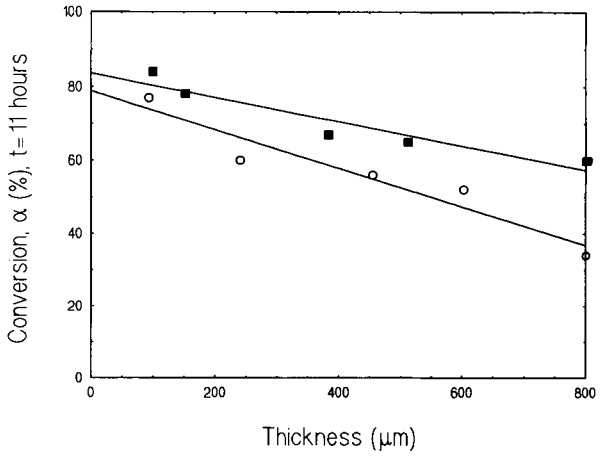

Figure 5 Plots of the degree of conversion α at a cure time t = 11 h as a function of the specimen thickness d for the CTV1 (○) and the CTV2 (■) formulations.

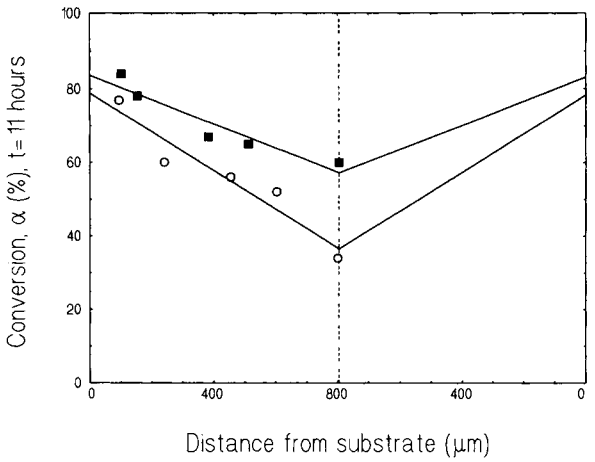

Figure 6 Plots of the complete cure profiles obtained from Figure 5 for the CTV1 (○) and the CTV2 (■) formulations.

The experimental setup is such that the cure emanates downward from the iron substrate toward the IRE. Since d_p is of the order of microns, only the material adjacent to the IRE is probed using this method (for a given θ and n_{21}). Thus, this technique is effectively equivalent to observing the chemical changes occurring in the vicinity of the halfway point in a bondline situation where the cure has emanated from two flanking iron substrates instead of one as is the case in this infrared experiment. We may thus obtain a *cure profile* of a bondline created using two active substrates that simulates accurately the way in which these adhesives are used in practice. The cure profile is defined as the variation of α with d from two substrates. Assuming identical substrates the cure profile of one half of a bondline will be the mirror image of the other half. The cure profiles for CTV1 and CTV2 are presented in Figure 6. It is apparent from Figure 6 that each half of the cure profile for CTV1 and CTV2 has the approximate shape of a linear gradient. This observation emphasizes the shortcomings of the crude model previously reported by us,[27] which relied on measurements from a complete bondline and which necessitated certain assumptions regarding the geometry of the bulk adhesive. The existence of a *cure gradient* emanating from each active substrate represents a more refined model.[28,29]

The cure through a bondline or CTV performance of the formulations CTV1 and CTV2 may be quantitatively compared by characterizing this cure gradient. The experimental data for each half of the profile is fitted to a straight-line equation (Fig. 5). We define two parameters that characterize the adhesives performance. The *CTV index* is the magnitude of the slope of one half of a profile and the *zero gap conversion (ZGV)* is the intercept of the α axis at $d = 0$ μm, that is, the conversion at zero gap (bondline thickness). Theoretically, a material that exhibits complete CTV will have a CTV index = 0 and a ZGV = 100%. Alternatively, a material exhibiting incomplete CTV will have a CTV index > 0 and a ZGV < 100%. Table I presents these calculated parameters along with some adhesive bond strength data that have been presented elsewhere.[29]

The bond strength data in Table I highlights the superior CTV performance of CTV2 over CTV1 at 500 μm gap and the equivalent CTV performance of both at 0 μm gap (effectively 5–10 μm in practice). The calculated CTV parameters are in satisfactory agreement with this trend. The CTV index of CTV2 (3.28×10^{-2}) is significantly lower than CTV1 (5.26×10^{-2}) whereas the ZGVs are broadly equivalent, 83.6% versus 78.9% for CTV2 and CTV1, respectively. This analysis of the data illustrates the usefulness of this technique as an analytical tool for the investigation and the quantification of the CTV performance of the various surface-initiated anaerobic adhesives.

Table I Calculated Cure Gradient Parameters and Bond Strength Data for the CTV1 and CTV2 Formulations

Formulation	Primer[a]	CTV Index ($\times 10^{-2}$)	ZGC[b] (%)	Bond Strength[c] (MPa)	
				0-μm gap	500-μm gap
CTV1	None	5.26	78.9	24.4	3.1
CTV2	N (Cu)	3.28	83.6	24.9	20.0

[a] For details see the experimental section.
[b] Zero gap conversion.
[c] Tensile testing according to ASTM D100-64.

Dielectric Spectroscopy Measurements

Here the properties of the observed cure gradient are investigated further. The method of dielectric spectroscopy is employed to analyze the complete cure profile through the bulk of the isothermally cured anaerobic adhesives, which have been cured from two identical substrates (as opposed to one in the infrared experiments). The background behind this analysis is given below.

The complete profile of the bondline from 0 to d is divided up into a very large number of segments of identical geometry. It is inferred from the observed cure gradient that each segment possesses a degree of conversion α that depends on d, for example, $\alpha = \alpha_{max}$ at $d = 0$ and $d = d$, and $\alpha = \alpha_{min}$ at $d = d/2$. This may be represented electrically as a large number of parallel RC circuits in series (Fig. 7). Here $n = 3, 4, \ldots, C_n > C_{n-1}$ and $R_n < R_{n-1}$, where C is the capacitance and R is the resistance. The following conditions also apply:

By definition,

$$C = \varepsilon' C_0 \tag{4}$$

where ε' is the real part of the complex permittivity $\varepsilon(\omega)$, C_0 is the geometrical capacitance, and ω is the angular frequency ($\omega = 2\pi f$). Thus

$$\varepsilon'_n > \varepsilon'_{n-1} \tag{5}$$

Also, by definition

$$R = \frac{1}{\omega C_0 \varepsilon''} \tag{6}$$

Thus

$$\varepsilon''_n > \varepsilon''_{n-1} \tag{7}$$

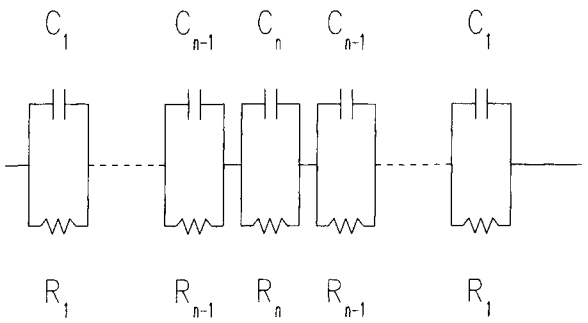

Figure 7 The electrical circuit interpretation of the cure profile in isothermally cured anaerobic adhesive formulations where $n = 3, 4, 5, \ldots, C$ is the capacitance and R is the resistance.

where ε'' is the dissipativity. The relaxation times of each RC element of the circuit obey Eq. (8):

$$\tau_n < \tau_{n-1} \tag{8}$$

The dielectric measurements taken here concern the complete symmetrical cure profile. The RT-FTIR results demonstrate that the cure profile of the heterogeneous three-dimensional molecular network can be approximated to a linear cure gradient emanating from each substrate into the bulk adhesive. This observed cure profile is symmetrical about the center of the adhesive bondline. Thus, the measured dielectric relaxation will correspond to a sample with a symmetrical distribution of relaxation times. As such, we select the empirical equation of Cole and Cole[30] to fit the data. The Cole–Cole equation describes the dielectric behavior arising from the existence of a symmetrical distribution of relaxation times, each of which alone would give rise to the Debye[41] (single relaxation time model) type of behavior. Indeed, the sample argand plots of ε' and ε'' (the so-called Cole–Cole plot) illustrated in Figure 8 reveal a symmetrical depressed (center below the ε' axis) semicircle with considerable broadening, which is suited to the Cole–Cole treatment. The Cole–Cole equation is written as:

$$\varepsilon(\omega) = \varepsilon_\infty + \frac{\varepsilon_{st} - \varepsilon_\infty}{1 + (i\omega\tau_m)^a} \tag{9}$$

where $\varepsilon(\omega)$ is the complex permittivity, ε_∞ is the high frequency ($\omega = \infty$) permittivity, ε_{st} is the static ($\omega = 0$) permittivity, and $i = \sqrt{-1}$. The Cole–Cole function exhibits a distribution of relaxation times about a mean relaxation time τ_m. The parameter a characterizes the slope of a tangent at the two points of intersection of the depressed semicircle with the ε' axis and $0 \leq a \leq 1$. a is a measure of the distribution of relaxation times where broad distributions are described by small values for a. The Debye[41] single relaxation time model has $a = 1$. The term $(\varepsilon_{st} - \varepsilon_\infty)$ is termed as the dielectric relaxation strength $\Delta\varepsilon$ and is proportional to the number density of dipoles taking part in the relaxation process. In the case of polymers exhibiting a nonsymmetrical distribution of relaxation times, the empirical equation of Havriliak and Negami[42] is widely employed to fit the dielectric relaxation data. This formalism is inappropriate here.

One of the undesirable features of the poor CTV situation is the presence of a large amount of gel of relatively low viscosity in the bulk of a cured specimen. This feature enhances the potential dipolar

mobility in the system. This is manifested by a relatively low value for τ_m and relatively high values for $\Delta\varepsilon$ and a. Figures 9 and 10 illustrate the experimentally obtained ε'' (symbols) and the fitted ε'' (dashed lines) as a function of frequency for CTV1 and CTV2, respectively. The fitting parameters are presented in Table II. The ε'' peak is observed to shift to higher frequencies, to increase in magnitude, and to decrease in half-width for greater sample thicknesses. This observation is consistent with the predictions made above, as increasing the specimen thickness generally decreases the CTV in an anaerobic acrylic adhesive material. Further analysis of Figures 9 and 10 confirms that CTV2 appears to exhibit better CTV than CTV1, for example, the ε'' peak associated with a 1380-μm sample of CTV2 is similar to the ε'' peak of a 716-μm CTV1 sample.

These findings are elucidated by plotting the calculated fitting parameters τ_m, $\Delta\varepsilon$, and a as a function of the sample thickness d (Figs. 11, 12, and 13). A decrease in τ_m and an increase in both $\Delta\varepsilon$ and a with greater d is observed. The plots also reveal that these parameters are significantly more sensitive to increases in d in formulation CTV1 than CTV2. We conclude from this analysis that CTV2 exhibits better CTV than CTV1. These results are in satisfactory agreement with the infrared spectroscopy and the tensile testing data in Table I, and they demonstrate the usefulness of this particular spectroscopic technique in the study of CTV in anaerobic adhesives.

We note from these measurements and calculations that the fitting parameters τ_m, $\Delta\varepsilon$, and a are sensitive to the degree of cure heterogeneity or the CTV performance in the model systems under investigation here. Since the main object of this work was to develop powerful techniques suited to the study of the *heterogeneous cure* in acrylic systems, the investigation of the relationship between these physical parameters and the chemical structure of the cured networks is inappropriate at this stage. The model systems are dominated by essentially the same cure chemistry with the exception of the organic salt BPH in CTV2. In light of the proprietary nature of BPH and other formulation components, no detailed account of the chemistry of these thermosetting systems is given here.

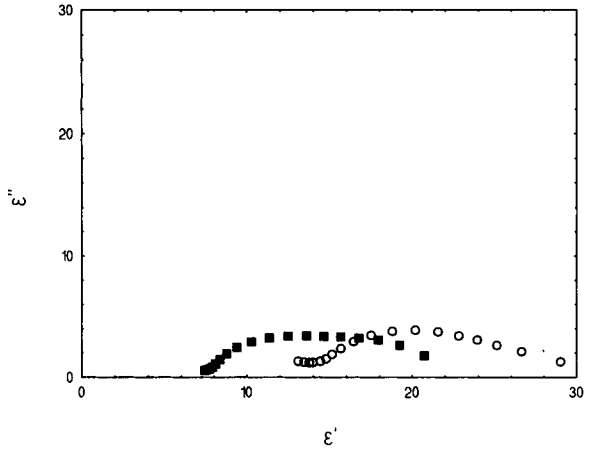

Figure 8 Argand plots for a 716-μm thick CTV1 sample (○) and a 1380-μm thick copper primed CTV2 sample (■).

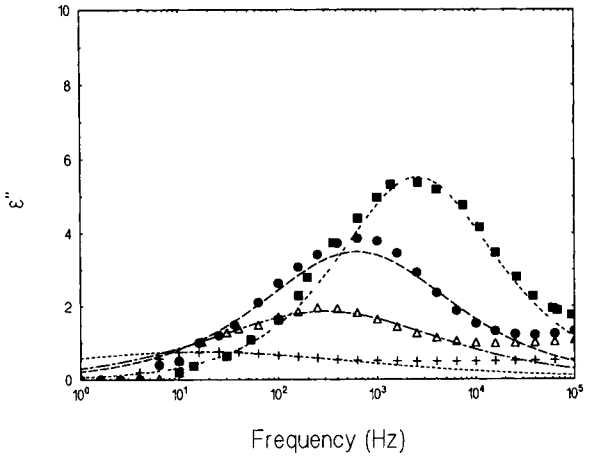

Figure 9 Plots of the experimental (symbols) and the fitted (dashed lines) dissipativity ε'' as a function of frequency for the CTV1 formulation at different sample thicknesses: (■) 1056 μm, (●) 716 μm, (△) 280 μm, and (+) 84 μm.

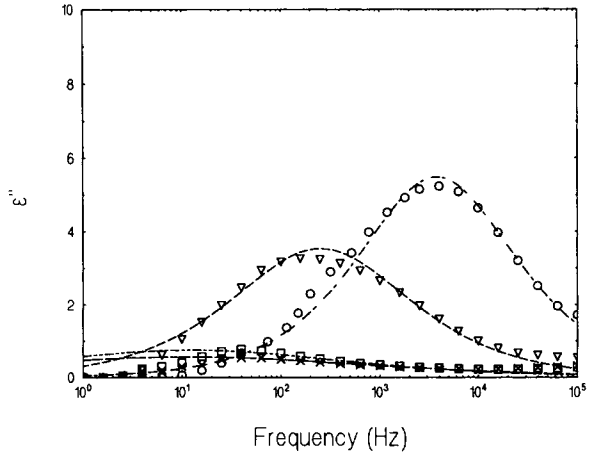

Figure 10 Plots of the experimental (symbols) and the fitted (dashed lines) dissipativity ε'' as a function of frequency for the CTV2 formulation at different sample thicknesses; (○) 2363 μm, (▽) 1380 μm, (□) 710 μm, and (×) 300 μm.

Table II Calculated Cole–Cole Fitting Parameters for the CTV1 and CTV2 Formulations

Formulation	Primer[a]	d (μm)	τ_m ($\times 10^{-5}$ s)	$\Delta\varepsilon$	a
CTV1	None	84	1020.0	5.14	0.36
CTV1	None	280	53.2	8.61	0.52
CTV1	None	716	25.6	13.52	0.61
CTV1	None	1011	6.2	18.02	0.70
CTV2	N (Cu)	300	1390.0	4.12	0.34
CTV2	N (Cu)	710	1300.0	4.62	0.40
CTV2	N (Cu)	1380	63.2	12.94	0.64
CTV2	N (Cu)	2363	4.2	15.06	0.70

[a] For details see the experimental section.

CONCLUSIONS

We have developed a technique based on RT-FTIR in the ATR mode that provides useful information on the nature of the cure profile in isothermally cured surface-initiated anaerobic acrylic adhesives. The profile of the two formulations investigated, CTV1 and CTV2, was found to approximate a linear cure gradient. The CTV performance of these two formulations was quantified by calculating and comparing the fitting parameters that were appropriate to each cure gradient: the CTV index, which is the magnitude of the slope, and the zero gap conversion (ZGC), which is the degree of conversion of monomeric units to polymer chains at zero gap. Using these criteria the CTV performance of CTV2 was found to be significantly better than in CTV1. This result was in satisfactory agreement with some previously quoted tensile testing data, cf. Table I.

The concept of a cure gradient existing in these samples was probed further using dielectric spectroscopy. Here, the observed dielectric relaxations were fitted to the Cole–Cole empirical expression. This formalism was selected because it is well established for fitting dielectric relaxation data that exhibit a broad symmetrical distribution of relaxation times. The fitting parameters of this expression were calculated and subsequently analyzed as a function of the sample thickness. It was found that the observed dependence of these parameters on the sample thickness was systematic. Furthermore, the observed trends in these data also indicated that CTV2 exhibits significantly better CTV performance than CTV1—results that were in satisfactory agreement with those obtained using infrared spectroscopy and tensile testing. These results thus provide further evidence to support our concept of a cure profile that takes the form of a cure gradient

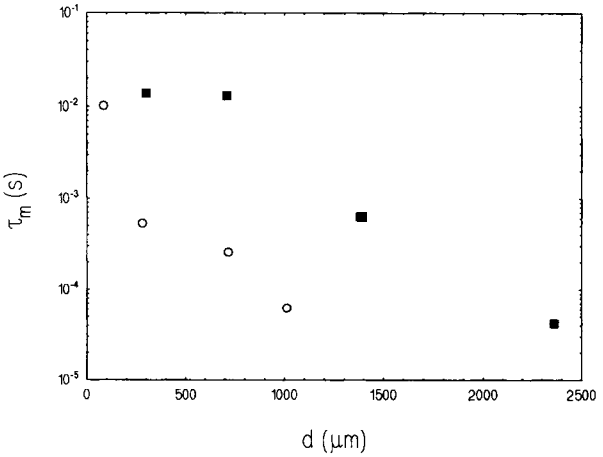

Figure 11 Plot of the fitted mean relaxation time τ_m as a function of the sample thickness d for the CTV1 (○) and the CTV2 (■) formulations.

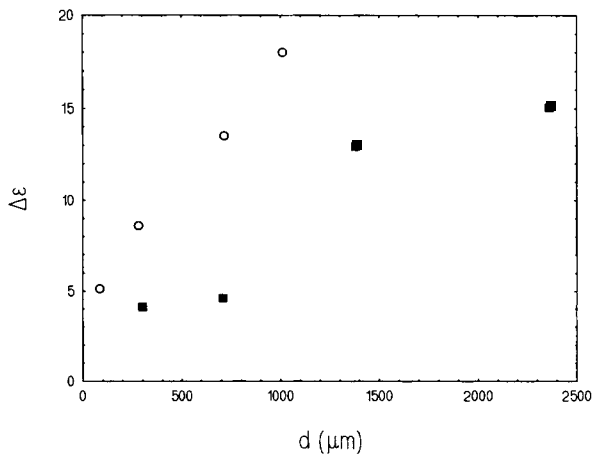

Figure 12 Plot of the fitted dielectric strength $\Delta\varepsilon$ as a function of the sample thickness d for the CTV1 (○) and the CTV2 (■) formulations.

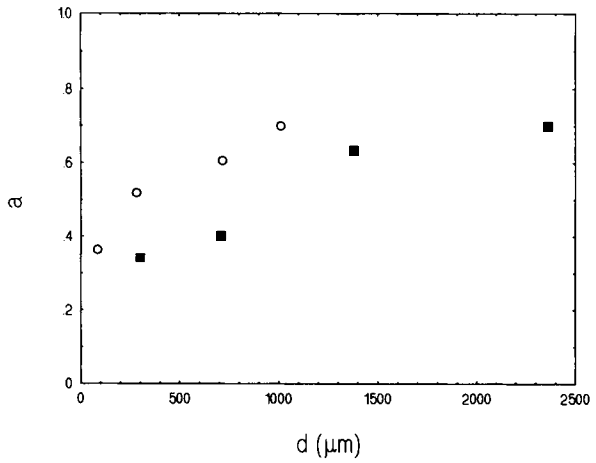

Figure 13 Plot of the fitted Cole–Cole distribution parameter a as a function of the sample thickness d for the CTV1 (○) and the CTV2 (■) formulations.

in isothermally cured surface-initiated anaerobic acrylics.

We have demonstrated the usefulness of the procedures outlined above as analytical tools for the study of heterogeneous cure or CTV in surface-initiated model anaerobic acrylic adhesives. While the application of infrared and dielectric spectroscopy to the study of thermoset cure is not new, these techniques have not been used previously in the investigation of heterogeneous cure in surface-initiated acrylics. Indeed, we propose that these methods would find useful practical application in the ascertainment of primary performance criteria as part of a comprehensive program for the development of actual high-performance anaerobic adhesives.

The authors wish to thank Professor G. P. Johari of McMaster University, Hamilton, Ontario, Canada, and Dr. J. Guthrie of Loctite (Ireland) Ltd. for useful discussions. We also thank Mr. B. Kennedy of Trinity College, Dublin, and Mr. J. Burke of Loctite (Ireland) Ltd. for technical assistance. The authors are grateful to Loctite (Ireland) Ltd. and to EOLAS for funding and for permission to publish this study.

REFERENCES

1. C. Decker and K. Moussa, *Makromol. Chem.*, **189,** 2381 (1988).
2. C. Decker and K. Moussa, *J. Polym. Sci.*, **28,** 3429 (1990).
3. C. Decker, in *Radiation Curing: Science and Technology,* S. P. Pappas, Ed., Plenum Press, New York, 1992, Chapter 4, p. 135.
4. C. Decker and K. Moussa, *Makromol. Chem.*, **191,** 963 (1990).
5. C. Decker and K. Moussa, in *Radiation Curing of Polymeric Materials,* E. Hoyle and J. F. Kinstle, Eds., American Chemical Society, Washington, DC, 1990, Chapter 31, p. 439.
6. S. J. Allen, S. J. Hardy, A. F. Jacobine, D. M. Glaser, B. Yang, and D. Wolf, *Euro. Polym. J.*, **26,** 1041 (1990).
7. S. J. Allen, S. J. Hardy, A. F. Jacobine, D. M. Glaser, B. Yang, D. Wolf, F. Catalina, S. Navaratnam, and B. J. Parsons, *J. Appl. Polym. Sci.*, **42,** 1169 (1991).
8. P. J. Brown, D. W. Wolf, and D. B. Yang, SME Technical Paper AD91-527, Proc. Adhesives '91, September 10–12, Atlanta, Georgia, 1991.
9. M. De Poortere, A. Ducarme, P. Dufour, and Y. Merck, *J. Oil Chem. Assoc.*, **61,** 195 (1978).
10. A. Van Neerbos, *J. Oil Chem. Assoc.*, **61,** 241 (1978).
11. S. Chambers, J. Guthrie, M. S. Otterburn, and J. Woods, *Polym. Comm.*, **27,** 209 (1986).
12. N. J. Harrick, *Internal Reflection Spectroscopy,* Interscience Publishers, New York, 1967.
13. J. Yarwood, *Anal. Proc.*, **30,** 13 (1993).
14. L. Fina and G. Chen, *Proc. Am. Chem. Soc., Div. Polym. Mat.: Sci. Eng.*, **64,** 38 (1991).
15. R. J. Jacobsen, in *Fourier Transform Infrared Spectroscopy,* Vol. 2, J. R. Ferraro and L. J. Basile, Eds., Academic Press, London, 1979, Chapter 5, p. 165.
16. H. Ishida, *Rubber Chem. Tech.*, **60**(3), 497 (1987).
17. T. NGuyen, E. Byrd, and C. Lin, *J. Adhesion Sci. Technol.*, **5**(9), 697 (1991).
18. S. D. Senturia and N. F. Sheppard, *Adv. Polym. Sci.*, **80,** 3 (1986).
19. M. B. M. Mangion and G. P. Johari, *J. Polym. Sci.*, **29,** 1127 (1991).
20. M. G. Parthun and G. P. Johari, *J. Polym. Sci.*, **30,** 655 (1992).
21. M. Wang, J. P. Szabo, and G. P. Johari, *Polymer,* **33**(23), 4951 (1992).
22. M. G. Parthun and G. P. Johari, *Macromolecules,* **25,** 3149 (1992).
23. M. Wang, G. P. Johari, and J. S. Szabo, *Polymer,* **33**(22), 4747 (1992).
24. C. G. Delides, D. Hayward, R. A. Pethrick, and A. S. Vatalis, *Eur. Polym. J.*, **28**(5), 505 (1992).
25. C. G. Delides, D. Hayward, R. A. Pethrick, and A. S. Vatalis, *J. Appl. Polym. Sci.*, **47,** 2037 (1993).
26. G. M. Maistros, H. Block, C. B. Bucknall, and I. K. Partridge, *Polymer,* **33**(21), 4470 (1992).
27. C. McArdle, J. Burke, and B. McGettrick, *Plastics, Rubber & Comp. Proc. and Appl.*, **16,** 245 (1991).
28. B. P. McGettrick and J. K. Vij, *Ferroelectrics,* **133,** 151 (1992).
29. B. P. McGettrick, J. K. Vij, and C. B. McArdle, *Polymer,* to appear.
30. R. H. Cole and K. S. Cole, *J. Chem. Phys.*, **9,** 341 (1941).
31. C. W. Boeder, in *Structural Adhesives—Chemistry and*

Technology, S. R. Hartshorn, Ed., Plenum Press, New York, 1986, Chapter 5.
32. D. J. Stamper, *Brit. Polym. J.,* **15,** 35 (1983).
33. Y. Okamoto, *J. Adhesion,* **32,** 227 (1990).
34. Y. Okamoto, *J. Adhesion,* **32,** 237 (1990).
35. M. R. Horner, Ph.D. Thesis, University of Cincinnatti, 1991.
36. J. M. Blanding, C. L. Osburn, and S. L. Watson, *J. Radiation Curing,* **5,** 13 (1978).
37. J. A. Brydson, in *Plastics Materials,* 4th ed., Butterworth Scientific, London, 1987, Chapter 15, p. 380.
38. B. Yang, *J. Polym. Sci.,* **31,** 199 (1993).
39. F. Kremer, D. Boese, G. Meier, and E. W. Fischer, *Progr. Coll. Polym. Sci.,* **80,** 129 (1989).
40. E. J. C. Kellar, G. Williams, V. Krongauz, and S. Yitchaik, *J. Mater. Chem.,* **1**(3), 331 (1989).
41. P. Debye, *Polar Molecules,* Chemical Catalogue Co., New York, 1929.
42. S. Havriliak and S. Negami, *J. Polym. Sci.; (C), Polym. Symp.,* **14,** 99 (1966).

Received July 22, 1993
Accepted October 12, 1993